

Electrochemical properties of $\text{GdBaCo}_{2/3}\text{Fe}_{2/3}\text{Cu}_{2/3}\text{O}_{5+\delta}$ –CGO composite cathodes for solid oxide fuel cell

Seung Jun Lee, Dong Seok Kim, Seung Hwan Jo, P. Muralidharan, Do Kyung Kim *

Department of Materials Science and Engineering, Korea Advanced Institute of Science and Technology (KAIST), 335 Gwahak-ro, Yuseong-gu, Daejeon 305-701, Republic of Korea

Available online 25 May 2011

Abstract

The composite cathodes of double-perovskite structure of $x\text{wt.}\% \text{Ce}_{0.9}\text{Gd}_{0.1}\text{O}_{1.95}$ (CGO)– $(100 - x)\text{wt.}\% \text{GdBaCo}_{2/3}\text{Fe}_{2/3}\text{Cu}_{2/3}\text{O}_{5+\delta}$ (FC-GBCO), where $x = 0, 10, 20, 40$ and 50 , were synthesized via a citrate combustion method followed by an organic precipitant method. The thermal-expansion coefficient (TEC) and electrochemical performance of the oxides were investigated as potential cathode materials for intermediate-temperature solid oxide fuel cells (IT-SOFCs). The TEC exhibited by composite cathode made of $40\text{ wt.}\% \text{CGO}$ – $60\text{ wt.}\% \text{FC-GBCO}$ (CG40) up to 900°C is $13.7 \times 10^{-6}^\circ\text{C}^{-1}$, which is lower value than FC-GBCO ($16.3 \times 10^{-6}^\circ\text{C}^{-1}$). The composite cathode of CG40 coated on $\text{Ce}_{0.9}\text{Gd}_{0.1}\text{O}_{1.95}$ electrolyte showed the lowest area specific resistance (ASR) i.e., $0.041 \Omega \text{ cm}^2$ at 750°C . An electrolyte supported ($300 \mu\text{m}$ thick) single-cell configuration of CG40/CGO/Ni-CGO attained a maximum power density of 800 mW cm^{-2} at 800°C . The unique composite composition of CG40 exhibited enhanced electrochemical performance, reduced TEC and good chemical compatibility with CGO electrolyte compared with their FC-GBCO cathode for IT-SOFCs.

© 2011 Elsevier Ltd and Techna Group S.r.l. All rights reserved.

Keywords: B. Composites; D. Perovskites; E. Electrodes; E. Fuel cells

1. Introduction

Recently, solid oxide fuel cells (SOFCs) have attracted as one of the most promising electrochemical energy conversion device because of high power efficiency, low pollutant emission and fuel flexibility [1–3]. Lowering operation temperature to intermediate temperature (600 – 800°C) is one of the main goals in the SOFC field [4,5]. A reduced operating temperature can extend the choice of materials, enhance the thermal stability of SOFC by minimizing thermal stresses experienced by the components during temperature cycling. However, the electrochemical activity of the cathode dramatically decreases with decreasing temperature and thus cathode becomes the limiting factor in determining the overall cell performance [4–6]. Therefore, the development of new electrodes with high electro-catalytic activity for the oxygen-reduction reaction is significant for intermediate-temperature solid-oxide fuel.

Recently, the mixed ionic-electronic conductors (MIECs) $\text{GdBaCo}_2\text{O}_{5+\delta}$ have been developing to be attractive potential cathode materials for IT-SOFCs [6–8]. This material exhibits high ionic conductivity due to the oxygen vacancies and high electronic conductivity [6–9]. Although very promising results were reported, double-perovskite oxides have high TEC that are not compatible with electrolyte materials [6,8,9]. The thermal expansion mismatch can cause thermal stress at interface of electrolyte and cathode and thus results in its long-term stability performance. More recently, our group have reported that Co site doped GBCO exhibits lower TEC and enhancement of electrochemical performance [8]. However, a further investigation on the optimization of TEC and electrochemical performance is necessary for the double-perovskite oxides to be used as potential cathodes in IT-SOFCs.

In order to improve cathode performance, the composite cathodes are of great interest that includes mixtures of cathode and ionic conducting materials [3,5,10–12]. The second phase, doped ceria in the cathode can expand the triple-phase boundaries (TPB) at which the oxygen reduction reaction occur from the two-dimensional interface between the electrolyte and the cathode to the entire zone of the cathode

* Corresponding author. Tel.: +82 42 350 4118; fax: +82 42 350 3310.

E-mail address: dkkim@kaist.ac.kr (D.K. Kim).

[3,10]. And composite cathode also can reduce mismatch in TEC between the electrolyte and cathode materials [9,10].

In order to improve the electrochemical performance and reduce TEC mismatch between cathode and electrolyte, we investigate composite cathode with Co site doped GBCO and CGO. In this study, the homogeneous xwt.% $\text{Ce}_{0.9}\text{Gd}_{0.1}\text{O}_{1.95}$ (CGO)–(100 – x)wt.% $\text{GdBaCo}_{2/3}\text{Fe}_{2/3}\text{Cu}_{2/3}\text{O}_{5+\delta}$ (FC-GBCO) composite cathodes, where $x = 0$ –50, were synthesized and area specific resistances (ASR) were studied by an electrochemical impedance spectroscopy technique. A single-cell performance of CG40 was also investigated.

2. Experimental

Initially, a double-perovskite oxide of $\text{GdBaCo}_{2/3}\text{Fe}_{2/3}\text{Cu}_{2/3}\text{O}_{5+\delta}$ (FC-GBCO) was synthesized via a citrate combustion method. Analytical grade $\text{Gd}(\text{NO}_3)_3 \cdot 6\text{H}_2\text{O}$ (>99.9%), $\text{Ba}(\text{NO}_3)_2$ (99+%), $\text{Co}(\text{NO}_3)_2 \cdot 2.5\text{H}_2\text{O}$ (98+%), $\text{Fe}(\text{NO}_3)_3 \cdot 9\text{H}_2\text{O}$ (99+%), and $\text{Cu}(\text{NO}_3)_2 \cdot 6\text{H}_2\text{O}$ (99+%) were used as precursors for the synthesis of oxide powders, and citric acid (99%) was used as fuel for the combustion reaction. Detailed synthesis of $\text{GdBaCo}_{2/3}\text{Fe}_{2/3}\text{Cu}_{2/3}\text{O}_{5+\delta}$ cathode for this investigation is available our previous report [3].

The stoichiometric amount of $\text{Ce}(\text{NO}_3)_3 \cdot 6\text{H}_2\text{O}$ (99.9%), $\text{Gd}(\text{NO}_3)_3 \cdot 6\text{H}_2\text{O}$ (99.9%) were dissolved in 50 ml of ethanol to form calculated xwt.% $\text{Ce}_{0.9}\text{Gd}_{0.1}\text{O}_{1.95}$ in composite. To the above clear solution, (100 – x)wt.% of calcined FC-GBCO powder was dispersed under sonication for 2 h. The $(\text{C}_2\text{H}_5)_2\text{NH}$ (diethylamine, 99.9%) precipitant was used to precipitate the CGO in the presence of FC-GBCO to form the composite. Thus, obtained composite powders were dried and calcined at 900 °C for 10 h. The composite cathodes have a composition varying from 0 to 50 wt.% CGO, and are named as CG0 to CG50.

The phase of synthesized powders was characterized with an X-ray diffractometer (XRD) (Rigaku, D/MAX-IIIIC X-ray diffractometer). The TEC for each rectangular-shape pellets sintered at 1000 °C for 2 h was measured using a dilatometer (NETZSCH DIL402C) from 30 to 900 °C. The cross-sectional

microstructure of the cathode coated on the CGO pellet was characterized by a scanning electron microscope (FE-SEM Philips XL30 FEG).

AC impedance spectroscopy of the symmetrical cell was tested under open-circuit conditions using an impedance spectroscopy (Solartron 1260 impedance/Gain-phase analyzer) in the frequency range of 10^6 – 10^{-2} Hz as a function of temperature (600–800 °C) in flowing air.

Single-cells were fabricated by screen printing NiO-CGO as the anode on one side of the dense CGO electrolyte pellet, and were sintered at 1300 °C for 2 h followed by CG40 cathode coating on the opposite side [8]. The single-cells were then sintered at 950 °C for 2 h. A Keithley 2400 sourcemeter was used to measure I – V polarization under flowing humidified H_2 (~3% H_2O) as fuel and air as oxidant.

3. Results and discussion

Fig. 1 shows the XRD patterns of FC-GBCO and CG40 cathode calcined at 900 °C for 10 h. For comparison, the patterns of GBCO and CGO are also shown in Fig. 1. It can be seen that the FC-GBCO oxide by the citric acid combustion method is single-phase, high crystalline double-perovskite structure with an orthorhombic structure, space group $Pmmm$ [8,13]. The unit cell parameters for FC-GBCO are $a = 3.885$ Å, $b = 3.884$ Å and $c = 7.636$ Å, and the cell volume is 115.252 Å³. The pattern of CG40 composite shows the presence of indexed peaks corresponding to CGO and GBCO without any other secondary phases. Thus, XRD result evidently indicates that CGO and $\text{GdBaCo}_{2/3}\text{Fe}_{2/3}\text{Cu}_{2/3}\text{O}_{5+\delta}$ have a good chemical compatibility as a homogeneous composite without forming any solid-solution.

Fig. 2 shows the thermal-expansion curves for different wt.% CG composites measured from 30 to 900 °C. The table in inset shows the calculated TEC values from the plots, which exhibits relatively reduced TEC compared with GBCO. Thus, substitution of Fe, Cu in the Co sites of GBCO can control the large thermal-expansion exhibited by GBCO [8]. As expected,

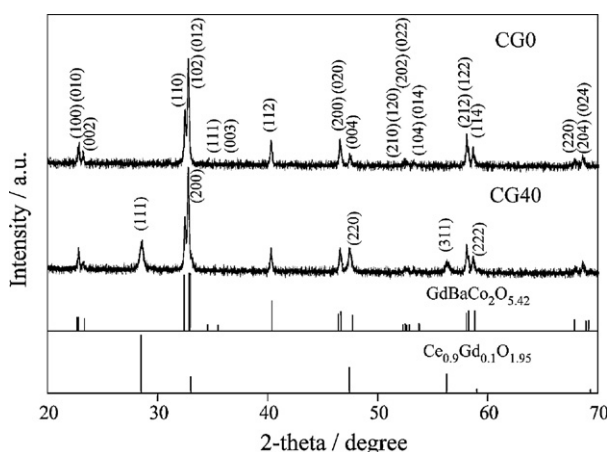


Fig. 1. XRD patterns of the CG0 and CG40 powders calcined at 900 °C for 10 h and compared with the JCPDS data of CGO and GBCO.

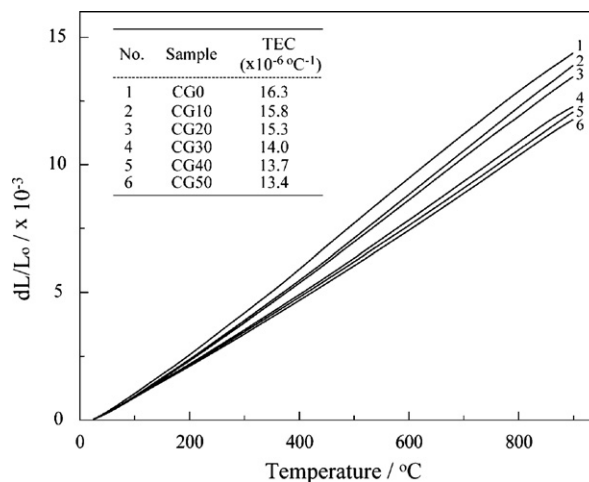


Fig. 2. Thermal-expansion (dL/L_0) curves of composite cathode in the temperature range of 30–900 °C in air. Inset table shows the calculated TEC values for composites cathode.

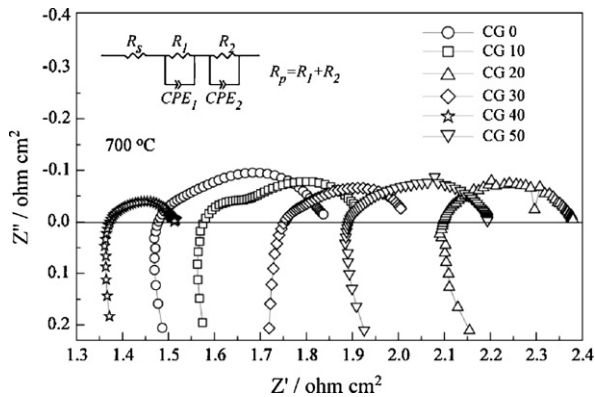


Fig. 3. Nyquist diagrams of the impedance spectroscopy for composite cathodes measured at 700 °C in air. Inset shows equivalent circuit for the composite cathode to fit the impedance curve.

a further decrease in the TEC values was observed by addition of CGO into FC-GBCO. For FC-GBCO cathode, the TEC of $16.3 \times 10^{-6} \text{ }^{\circ}\text{C}^{-1}$ decrease to $13.7 \times 10^{-6} \text{ }^{\circ}\text{C}^{-1}$ for CG40 cathode. The reduction of the TEC of composite cathode is mainly attributed to smaller TEC of CGO, for example, the TEC of CGO is $11.5 \times 10^{-6} \text{ }^{\circ}\text{C}^{-1}$ in the temperature range of 300–1050 K in air [14].

The performance of composite cathode sintered at 950 °C for 2 h was investigated by AC impedance spectroscopy. Nyquist plots of the electrochemical impedance spectra from CG0 to CG50 at 700 °C are shown in Fig. 3 and the equivalent circuit for the analysis of the impedance data is illustrated in inset of Fig. 3. The resistivity ($R_p = R_1 + R_2$) was obtained by fitting the impedance spectrum with an equivalent circuit model using the nonlinear least squares fitting program of the Z-view software. The intercepts of the semicircle on the real axis at high-frequency region represent the total ohmic resistivity (R_s) of the electrolyte and lead wire, whereas the resistance between the two intercepts with the real axis corresponds to the area specific resistance (polarization resistance, R_p). It is obvious that the addition of an ionically conducting phase CGO to FC-GBCO cathode resulted in a significant reduction of the total interfacial polarization resistance, typically from $0.14 \text{ } \Omega \text{ cm}^2$ for FC-GBCO to less than $0.041 \text{ } \Omega \text{ cm}^2$ for CG40 at 750 °C.

The calculated log ASR of the different wt.% CG composites in Fig. 4 shows the interface resistances as a function of temperature. The inset (a) shows the plot of ASR values vs. different wt.% CG composites. The total interfacial polarization resistance (R_p) decreases as the CGO content increase up to 40 wt.%. The increased performance of composite cathodes can be explained to the following reason: the triple phase boundary (TPB) areas where oxygen reduction reaction is occurred were extended from the cathode/electrolyte interface to the three-dimensional bulk of the electrode, and thus significantly improve the cathode performance. As a result, the high ionic conductive CGO in CG composite cathodes may facilitate oxygen conduction path and greatly expand the electrochemical reaction zone to improve the performance [3,10]. A further increase in CGO concentration to higher than 50 wt.%, however, results in a higher interfacial polarization

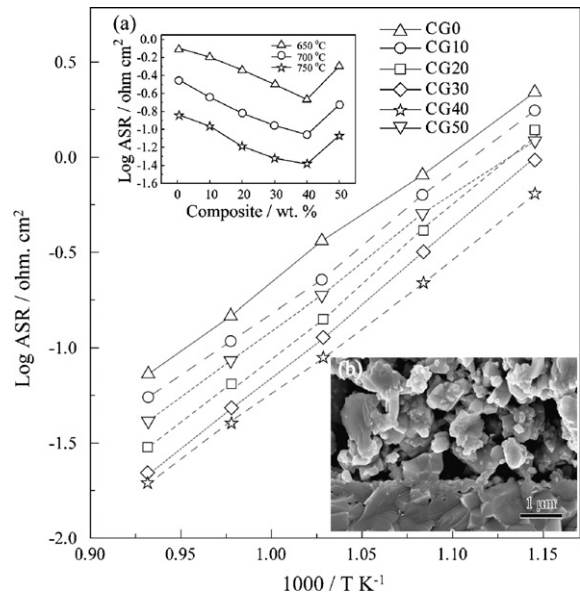


Fig. 4. plots of log ASR for the symmetrical half-cells of different wt.% CG/CGO at interface, measured in air. The insets (a) shows the ASR values vs. wt.% CG composites and (b) shows the SEM images of cross-sectional view of an interface between CG40 cathode and CGO electrolyte after cell test.

resistance. With the addition of CGO, the path for electronic transport may not be effectively built up, resulting in increase of polarization resistance [5,10,13]. Thus, the non-continuous path for electronic transport may lead to the high ohmic resistance of the composite cathode, which can increase the ohmic resistance with $x = 50 \text{ wt.}\%$.

The inset (b) in Fig. 4 shows the cross-sectional views of an interface between the CG40 cathode and the CGO electrolyte, after cell test. The SEM images expose a highly porous morphology that ensures good gas diffusion and presence of inter-connectivity at interfaces between the porous cathode and densified electrolyte without any cracking and/or delamination. It is observed that the composite cathode consists of

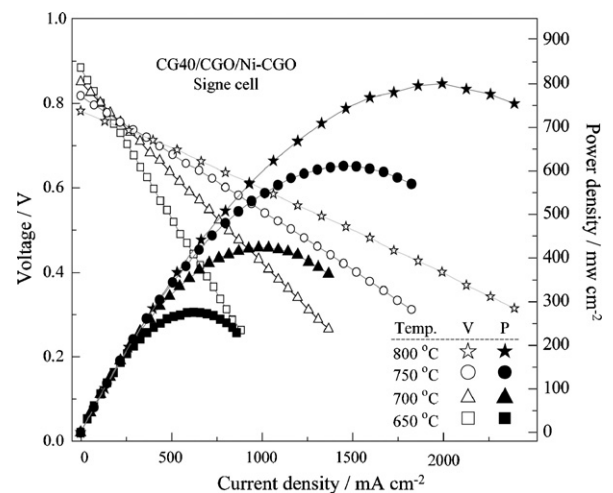


Fig. 5. Power density and voltage as a function of current density for single cell with CG40/CGO/Ni-CGO cell under humidified H_2 fuel and air oxidant at 650–800 °C.

homogeneously distributed nano-size (~ 100 nm) spherical CGO particles on the surface of the bottle-neck shaped FC-GBCO particles (~ 1 μm). This typical morphology may be one of the reasons for improved cathode performance during the oxygen reduction reaction. This partially supports the reason for enhancement of electrochemical performance of CG40 compared with pristine CGO.

Fig. 5 shows the power density and voltage as a function of current density for the electrolyte supported single-cell configuration of CG40/CGO/Ni-CGO cells using H_2 as the fuel and static air as the oxidant in the temperature range 650–800 $^\circ\text{C}$. The maximum power density values were 611 and 800 mW cm^{-2} at 750 and 800 $^\circ\text{C}$, respectively. These results demonstrate that CG40 exhibits high performance in the intermediate temperature regime than previous reports of double perovskite-type cathodes [4,6,9]. The cell performance is encouraging and suggests that CG40 is a potential cathode material for IT-SOFCs.

4. Conclusions

The different wt.% of CGO to CG50 composite cathodes was synthesized via citric acid combustion method followed by the precipitation method. The ASR values were improved by addition of nano-size CGO and FC-CBCO particles to form CG composite cathodes. The TEC value of CG40 is reduced to $13.7 \times 10^{-6} \text{ }^\circ\text{C}^{-1}$ by mixing nano-sized CGO. The reduced TEC may improve the thermal stability by achieving a match of the TEC between electrolyte and cathode. The CG40 showed the lowest area specific resistance (ASR) i.e., $0.041 \text{ } \Omega \text{ cm}^2$ at 750 $^\circ\text{C}$. The maximum power densities of the electrolyte supported single-cell configuration of CG40/CGO/Ni-CGO attained 611 and 800 mW cm^{-2} at 750 and 800 $^\circ\text{C}$, respectively. The achieved power density and reduced TEC are encouraging and indicate that Fe and Cu co-doped GBCO with 40 wt.% CGO composite cathode is a promising cathode material for IT-SOFCs.

Acknowledgements

This work was financially supported by the Priority Research Centers Program through the National Research Foundation of Korea (NRF) (No. 2009-0094041), Center for ERC Program (2008-0062206) and by Korea Science and

Engineering Foundation (KOSEF) grant (No. R01-2008-000-20480-0) funded by Korea government (MSET).

References

- [1] B.C.H. Steele, Appraisal of $\text{Ce}_{1-y}\text{Gd}_y\text{O}_{2-y/2}$ electrolytes for IT-SOFC operation at 500 $^\circ\text{C}$, *Solid State Ionics* 129 (2000) 95–110.
- [2] P. Muralidharan, S.H. Jo, D.K. Kim, Electrical conductivity of submicrometer gadolinia-doped ceria sintered at 1000 $^\circ\text{C}$ using precipitation-synthesized nanocrystalline powders, *Journal of the American Ceramic Society* 91 (2008) 3267–3274.
- [3] S.J. Lee, P. Muralidharan, S.H. Jo, D.K. Kim, Composite cathode for IT-SOFC: Sr-doped lanthanum cuprate and Gd-doped ceria, *Electrochemistry Communication* 12 (2010) 808–811.
- [4] Q. Zhou, T. He, Q. He, Y. Ji, $\text{SmBaCo}_2\text{O}_{5+\delta}$ double-perovskite structure cathode material for intermediate-temperature solid-oxide fuel cells, *Journal of Power Sources* 185 (2008) 754–758.
- [5] H. Gu, H. Chen, L. Gao, L. Guo, Electrochemical properties of $\text{LaBaCo}_2\text{O}_{5+\delta}\text{--Sm}_{0.2}\text{Ce}_{0.8}\text{O}_{1.9}$ composite cathodes for intermediate-temperature solid oxide fuel cells, *Electrochimica Acta* 54 (2009) 7094–7098.
- [6] J.-H. Kim, A. Manthiram, $\text{LnBaCo}_2\text{O}_{5+\delta}$ oxides as cathodes for intermediate-temperature solid oxide fuel cells, *Journal of the Electrochemical Society* 155 (2008) B385–B390.
- [7] A. Tarancón, A. Morata, G. Dezanneau, S.J. Skinner, J.A. Kilner, S. Estradé, F. Hernández-Ramírez, F. Peiró, J.R. Morante, $\text{GdBaCo}_2\text{O}_{5+\delta}$ layered perovskite as an intermediate temperature solid oxide fuel cell cathode, *Journal of Power Sources* 174 (2007) 255–263.
- [8] S.H. Jo, P. Muralidharan, D.K. Kim, Enhancement of electrochemical performance and thermal compatibility of $\text{GdBaCo}_{2/3}\text{Fe}_{2/3}\text{Cu}_{2/3}\text{O}_{5+\delta}$ cathode on $\text{Ce}_{1.9}\text{Gd}_{0.1}\text{O}_{1.95}$ electrolyte for IT-SOFCs, *Electrochemistry Communication* 11 (2009) 2085–2088.
- [9] Q. Zhou, F. Wang, Y. Shen, T. He, Performances of $\text{LnBaCo}_2\text{O}_{5+\delta}\text{--Ce}_{0.8}\text{Sm}_{0.2}\text{O}_{1.9}$ composite cathodes for intermediate-temperature solid oxide fuel cells, *Journal of Power Sources* 195 (2010) 2174–2181.
- [10] C. Zhu, X. Liu, D. Xu, D. Wang, D. Yan, L. Pei, T. Lü, W. Su, Electrochemical performance of $\text{Pr}_{0.7}\text{Sr}_{0.3}\text{Co}_{0.9}\text{Cu}_{0.1}\text{O}_{3-\delta}\text{--Ce}_{0.8}\text{Sm}_{0.2}\text{O}_{1.9}$ composite cathodes in intermediate-temperature solid oxide fuel cells, *Journal of Power Sources* 185 (2008) 212–216.
- [11] C. Fu, K. Sun, N. Zhang, X. Chen, D. Zhou, Electrochemical characteristics of LSCF-SDC composite cathode for intermediate temperature SOFC, *Electrochimica Acta* 52 (2007) 4589–4594.
- [12] Y.J. Leng, S.H. Chan, Q.L. Liu, Development of LSCF-GDC composite cathodes for low-temperature solid oxide fuel cells with thin film GDC electrolyte, *International Journal of Hydrogen Energy* 33 (2008) 3808–3817.
- [13] A. Maignan, C. Martin, D. Pelloquin, N. Nguyen, B. Raveau, Structural and magnetic studies of ordered oxygen-deficient perovskites $\text{LnBaCo}_2\text{O}_{5+\delta}$, closely related to the “112” structure, *Journal of Solid State Chemistry* 142 (1999) 247–260.
- [14] V.V. Kharton, A.V. Kovalevsky, A.P. Viskup, A.L. Shaula, F.M. Figueiredo, E.N. Naumovich, F.M.B. Marques, Oxygen transport in $\text{Ce}_{0.8}\text{Gd}_{0.2}\text{O}_{2-\delta}$ -based composite membranes, *Solid State Ionics* 160 (2003) 247–258.